Hexose permeation pathways in *Plasmodium falciparum*-infected erythrocytes

Charles J. Woodrow, Richard J. Burchmore, and Sanjeev Krishna*

Department of Infectious Diseases, St. George's Hospital Medical School, Cranmer Terrace, London SW17 ORE, United Kingdom

Edited by David Weatherall, University of Oxford, Oxford, United Kingdom, and approved June 21, 2000 (received for review April 5, 2000)

Plasmodium falciparum **requires glucose as its energy source to multiply within erythrocytes but is separated from plasma by multiple membrane systems. The mechanism of delivery of substrates such as glucose to intraerythrocytic parasites is unclear. We have developed a system for robust functional expression in *Xenopus* oocytes of the *P. falciparum* asexual stage hexose permease, PfHT1, and have analyzed substrate specificities of PfHT1. We show that PfHT1 (a high-affinity glucose transporter, $K_m \approx 1.0$ mM) also transports fructose ($K_m \approx 11.5$ mM). Fructose can replace glucose as an energy source for intraerythrocytic parasites. PfHT1 binds fructose in a furanose conformation and glucose in a pyranose form. Fructose transport by PfHT1 is ablated by mutation of a single glutamine residue, Q169, which is predicted to lie within helix 5 of the hexose permeation pathway. Glucose transport in the Q169N mutant is preserved. Comparison in oocytes of transport properties of PfHT1 and human facilitative glucose transporter (GLUT)1, an archetypal mammalian hexose transporter, combined with studies on cultured *P. falciparum*, has clarified hexose permeation pathways in infected erythrocytes. Glucose and fructose enter erythrocytes through separate permeation pathways. Our studies suggest that both substrates enter parasites via PfHT1.**

Plasmodium falciparum infection is responsible for more than two million deaths annually. *P. falciparum* depends on a continuous supply of host-derived glucose during the clinically important asexual stages of growth and replication within erythrocytes (1). A malarial hexose transporter (PfHT1) expressed during these asexual stages has recently been identified and functionally assayed in *Xenopus laevis* oocytes (2). *PfHT1* is a single copy gene with no close homologues and encodes a hexose transporter belonging to the major facilitator superfamily of proteins. PfHT1 has a relatively high affinity for glucose when compared with human facilitative glucose transporter (GLUT)1, the principal mammalian hexose transporter expressed in erythrocytes and endothelial cells lining the blood–brain barrier, as well as other cell types (3, 4). PfHT1 (localized by indirect immunofluorescence) is associated with intraerythrocytic parasites and is not exported to the host plasma membrane.

Analysis of substrate binding and transport properties of PfHT1 enhances our understanding of how malarial parasites obtain essential nutrients through three membrane systems, by focusing on the transport of glucose as a model substrate. Furthermore, mechanistic differences between PfHT1 and GLUT1, associated with individual structural and topological arrangements of each transporter, present enticing chemotherapeutic targets. We have adopted a number of methodologies to understand hexose transport by PfHT1, to establish differences in transport properties between PfHT1 and GLUT1, and to examine the delivery of hexoses to parasites within red cells.

Without high-resolution structural information on integral membrane proteins belonging to the major facilitator superfamily, indirect approaches to defining the substrate binding site are necessary. To optimize the *Xenopus* oocyte heterologous expression system for PfHT1, we tested plasmid constructs differing only in the presence of regions that may regulate translation in oocytes. We then used this system to examine an extended array of hexose analogues and to map critical positions that interact with PfHT1. This approach has been simultaneously applied to GLUT1 to allow direct comparison between parasite and mammalian transporters.

A complementary strategy to elucidate PfHT1 substrate–protein interactions is based on mutational analysis. This has already provided detailed mechanistic information when applied to other members of the major facilitator superfamily (5). We mutated a highly phylogenetically conserved residue in helix 5 of PfHT1 that has been intensively studied in homologues (6, 7). These findings combined with previous studies demonstrate topological conservation among hexose transporters but also confirm important mechanistic differences between phylogenetically diverse organisms.

Experimental Procedures

Site-Directed Mutations and Cloning of PfHT1. PCR on genomic DNA from parasite clone 3D7 by using *Pfu* polymerase (Stratagene) was initially carried out with primers faithful to wild-type sequence and the resulting product cloned into pGEM-T-easy (Promega). Subsequently we used primers with *Bgl*II restriction sites, with or without a strong eukaryotic Kozak consensus in the 5′ primer (AATAATG to CACCATG, where the initiation codon is underlined). Products were cloned into pUC 18 (Amersham Pharmacia Biotech) and subcloned into either pGEM-T-easy (Kozak-only construct) or into pSPGT1, which contains 5′ and 3′ untranslated *Xenopus* β-globin sequences (8) [Kozak/untranslated region (UTR) and UTR-only constructs]. For the Q169N mutant, complementary PCR primers were designed to introduce the appropriate mutation by standard methods (2). All constructs were verified by sequence analysis.

Expression of PfHT1 and GLUT1 in *Xenopus* Oocytes and Kinetic Analyses. *X. laevis* oocytes were assayed as described previously (9). cRNA for PfHT1 or GLUT1 (8) was transcribed (MEGAscript T7 or SP6, Ambion, Austin, TX) from linearized templates and oocytes injected with cRNA (10 ng in 25 nl of water) or RNase-free water. All studies were carried out 18–96 h after microinjection. For kinetic studies, uptake rates of permeant D-[U-^{14}C]glucose (310 mCi·mmol^{-1}), 2-deoxy-D-[U-^{14}C]glucose (2-DOG) (58 mCi·mmol^{-1}), D-[U-^{14}C]fructose (289 mCi·mmol^{-1}) from Amersham and 3-*O*-[^{14}C]methyl-D-glucose (50 mCi·mmol^{-1}) from ICN were measured after 5–20 min incubation at room temperature and were corrected for uptake into water-injected controls. Linear uptake of substrates was confirmed for all incubation times and for each range of

This paper was submitted directly (Track II) to the PNAS office.

Abbreviations: 2,5-AHM, 2,5-anhydro-D-mannitol; DHA, dehydroascorbic acid; DOG, deoxy-D-glucose; GLUT, human facilitative glucose transporter; K_i, half-maximal inhibition constant for carrier transport; PfHT1, *Plasmodium falciparum* hexose transporter 1; UTR, untranslated region; 3-OMG, 3-*O*-methyl-D-glucose.

*To whom reprint requests should be addressed. E-mail: s.krishna@sghms.ac.uk.

The publication costs of this article were defrayed in part by page charge payment. This article must therefore be hereby marked "*advertisement*" in accordance with 18 U.S.C. §1734 solely to indicate this fact.

Article published online before print: *Proc. Natl. Acad. Sci. USA*, 10.1073/pnas.170153097. Article and publication date are at www.pnas.org/cgi/doi/10.1073/pnas.170153097

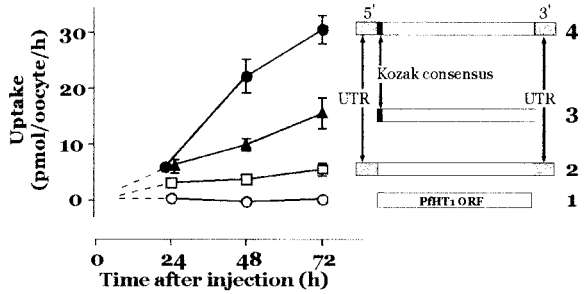

Fig. 1. Influence of untranslated sequences on expression of PfHT1 in *Xenopus* oocytes. Sequence modifications outside the ORF for PfHT1 are shown next to induced glucose uptake. Oocytes from a single toad were injected with RNA (5 ng) transcribed from different plasmid constructs and assayed for glucose uptake at the times indicated (six to eight oocytes per uptake; data displayed are mean ± SE). Constructs are: (1) PfHT1 ORF (open rectangle); (2) PfHT1 ORF with 5′ and 3′ UTRs from *Xenopus* β-globin (shaded); (3) PfHT1 ORF with Kozak consensus (filled); and (4) PfHT1 ORF with both UTRs and Kozak consensus. Data represent one of two independent experiments.

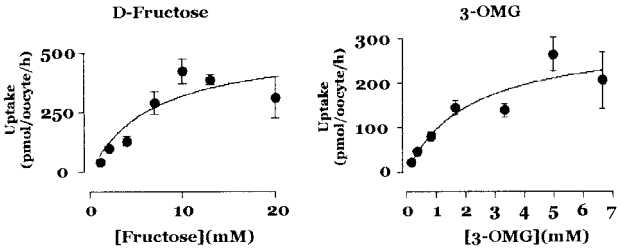

Fig. 3. Transport of fructose and 3-OMG by PfHT1. (*Left*) Initial uptake rates of D-fructose (representative of three independent experiments; see Table 2) and (*Right*) 3-OMG (representative of three independent experiments; see Table 1) are plotted against concentration of substrate (eight oocytes per concentration; mean ± SE). In this experiment, D-fructose K_m = 6.8 mM; for 3-OMG K_m = 0.9 mM.

experimental concentrations. Estimation of kinetic parameters was by nonlinear regression analysis by using a Michaelis–Menten model (PRISM Ver. 2, GraphPad, San Diego).

Studies with Competitors and Inhibitors. For studies with competitors and inhibitors (all from Sigma), uptakes were carried out for 20–30 min with radiolabeled permeant D-glucose (2.69 μM) and unlabeled D-glucose (35 μM) with variable amounts of competitor/inhibitor. The range of competitor concentrations used was determined in preliminary studies for each competitor. Data were analyzed by using nonlinear regression analysis with a one-site competition model and were corrected for uptake into water-injected control oocytes (PRISM). Dehydroascorbic acid (DHA) was dissolved, and assays were completed within 15 min to minimize loss through reduction (10).

Experiments on Cultured *P. falciparum*. Parasites (clone 3D7) were cultured (11) and routinely grown in 20 mM glucose. For experiments in low glucose, glucose-free RPMI was supplemented with D-fructose. Assays were carried out in sextuplicate at 1% hematocrit and 0.3% initial parasitemia by using asynchronous cultures. [^{3}H]Hypoxanthine (0.5 μCi/well) was added after 24 h in various concentrations of hexoses. Cells were harvested at 48 h and hypoxanthine incorporation measured by scintillation counting (11).

Results

Optimization of PfHT1 Expression. cRNA encoding native PfHT1 sequence induced low levels of glucose uptake in oocytes [(Fig. 1) up to two times that of water-injected control oocytes (4)]. Modifications were therefore made in UTRs by introducing a conserved eukaryotic Kozak consensus (CACCATG) before the start codon (underlined) or by inserting the ORF for PfHT1 into a vector containing 5′ and 3′ UTRs from *Xenopus* β-globin (gift of G. Gould). cRNA containing a strengthened Kozak sequence induced larger increases in glucose uptake than cRNA without the Kozak sequence but with 5′ and 3′ UTRs of *Xenopus* β-globin sequences (Fig. 1). A construct containing both modifications induced the highest glucose transport activity of all, as we have reported previously (2), and was used for all kinetic studies. Introduction of a Kozak consensus acts synergistically with the presence of 5′ and 3′ UTRs from *Xenopus* β-globin to optimize translational efficiency of RNA encoding PfHT1 in oocytes.

Kinetics of Substrate Transport. PfHT1 transports D-glucose, 2-DOG, 3-*O*-methyl-D-glucose (3-OMG), and D-fructose (see Fig. 2 for chemical structures and Fig. 3 for examples of

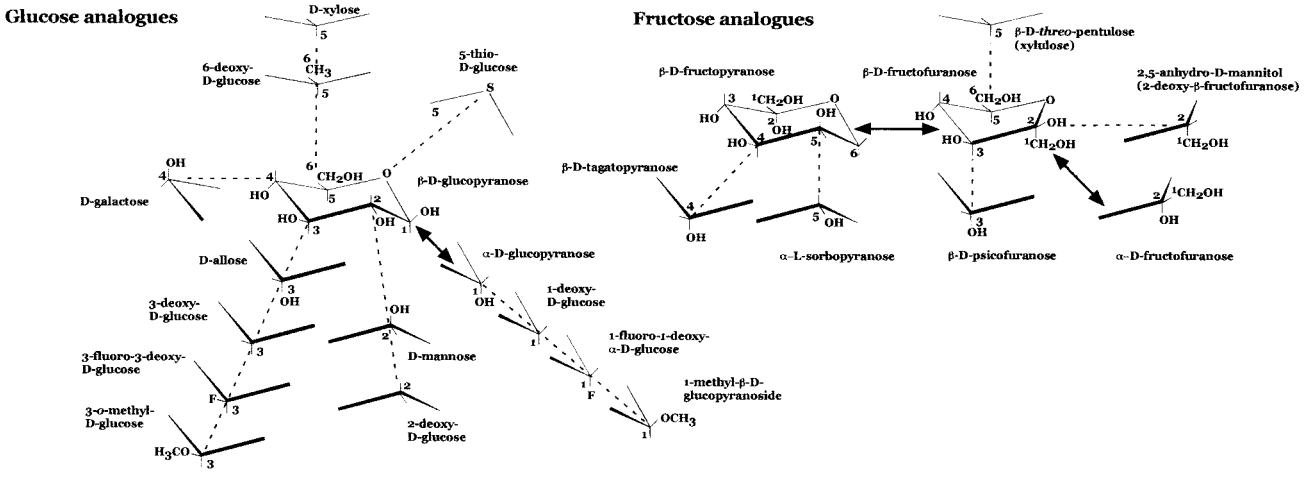

Fig. 2. Analogues used in studies on PfHT1 and GLUT1. Structures are represented as chair conformations. For glucose and fructose, solid arrows indicate interconversions occurring in solution. For analogues, a single common form is shown for simplicity. Percentages of analogues in each conformation at equilibrium in solution are shown in Table 2.

Table 1. Active analogue and K_m studies on PfHT1 and GLUT1

Substrate	PfHT1 K_i	GLUT1 K_i
Aldose analogues		
D-Glucose	$K_m = 1.0 \pm 0.2$*	$K_m = 2.3, 2.6$
C1 position		
1-Deoxy-D-glucose	14.7, 15.9	38.8, >50
1F-1-α-Deoxy-D-glucose	1.0, 1.6	1.3, 1.7
1F-1-β-Deoxy-D-glucose	1.0, 2.4	1.0, 5.2
1α-1-Methylglucopyranoside	>50	ND
1β-1-Methylglucopyranoside	>50	ND
C2 position		
2-Deoxy-D-glucose	$K_m = 1.3$ 0.9, 1.7	3.1, 6.3
D-Mannose	0.7, 1.1	1.4, 3.5
C3 position		
3-Deoxy-D-glucose	13.2, 16.8	>50
3-OMG	$K_m = 1.3 \pm 0.3$* $K_i = 1.4, 2.7$	30.8, 36.9
3-Fluoro-3-deoxy-D-glucose	1.6, 1.8	ND
D-Allose	22.0, 25.3	>50
C4 position		
D-Galactose	6.1, 7.9	25.2, 47.1
4,6-*O*-Ethylidene-α-D-glucose	>50	ND
C5 position		
5-Thio-D-glucose	2.7, 3.7	4.6, 6.9
C6 position		
6-Deoxy-D-glucose	2.2 ± 0.9*	15.0, 16.8
D-Xylose	16.1, 34.4	>50
Endofacial ligand		
Cytochalasin B	1.4, 4.3 μM	0.9 μM
Miscellaneous†	>50	ND

Values are in mM unless otherwise indicated. Independent replicate K_i values based on inhibition of D-glucose uptake are shown. The 6-DOG value for PfHT1 has been previously reported (2).
*Means ± SE of three independent experiments.
†Consists of D-mannitol, D-sorbitol, *myo*-inositol, sucrose, dehydroascorbic acid, glucose 6-phosphate, and maltose.

D-fructose and 3-OMG kinetics; K_m values are in Tables 1 and 2). Kinetic measurements for D-glucose and D-fructose were obtained in the same experiment, with resulting V_{max} values of 302 and 536 pmol/oocyte/min, respectively, giving ≈5-fold higher specificity (V_{max}/K_m) for glucose over fructose. This ability to transport both D-glucose and D-fructose distinguishes PfHT1 from mammalian glucose transporters, because although GLUT2 and GLUT5 transport fructose, they have low or no affinity for glucose.

Active Analogue Studies on PfHT1. Detailed characterization of substrate-transporter interaction utilized a series of hexose analogues as competitors for transport of D-glucose under zero-trans conditions (active analogue approach, Tables 1 and 2). Such K_i measurements may be affected by the differential rates of translocation between competitor and D-glucose. These K_i values therefore provide only an estimate of affinity between PfHT1 and competitor. At equilibrium in aqueous solution, five-membered (furanose) or six-membered (pyranose) ring structures of pentoses and hexoses are favored over the open form. Each ring can mutatrotate between two anomers: α and β (Fig. 2). Hence each hexose analogue potentially exists as four structures, any of which may interact with PfHT1 with differing affinity. Pyranose forms are favored by aldoses, with D-glucose existing as 33% α- and 66% β-anomer. In contrast, ketoses often show relatively high proportions of furanose forms.

Deoxyaldose Analogues. Use of DOG analogues provides an initial assessment of the overall importance of hydrogen bonding at each carbon position to PfHT1 (Table 1). In comparison with D-glucose, small increases in K_i (4-fold or less) are observed with 2-DOG, 5-thio-D-glucose, and 6-DOG. Removal of oxygen atoms from C1 or C3 positions is associated with much larger increases in K_i (>10-fold for 1-DOG and 3-DOG compared with the K_m for D-glucose), illustrating that hydroxyl groups in these positions are involved in high-affinity interactions with PfHT1.

Fluoro- and Methylaldohexoses. Introduction of a C1-fluorine atom fixes the D-glucose derivative as pyranose, with the fluorine atom (a strong hydrogen bond acceptor) in either α or β anomeric configuration. Compared with 1-DOG both 1-fluoro-1-deoxy-α- and 1-fluoro-1-deoxy-β-D-glucose almost restore K_i to that of D-glucose (Table 1), suggesting that both anomers can bind to PfHT1. Similarly, 3-fluoro-3-DOG has a K_i comparable to that of D-glucose, confirming hydrogen bonding at the C3 position.

1-α-Methylglucopyranoside and 1-β-methylglucopyranoside inhibited glucose uptake poorly (Table 1); methyl substitutions at C1 in either α or β configurations sterically hinder interaction with the hexose-binding site in PfHT1. In contrast, PfHT1 displays high-affinity transport of 3-OMG (Fig. 3), showing that

Table 2. Relative proportions of ketose forms and active analogue studies on PfHT1 and GLUT1

	% furanose		% pyranose			
Substrate	α	β	α	β	PfHT1 K_i	GLUT1 K_i
D-Fructose	6.5	25	2.5	65	$K_m = 11.5$* ± 1.6, $K_i = 10.6, 11.7$	>50
C2 position						
2,5-AHM		100			1.4 ± 0.3*	>50
C3 position						
D-Psicose	39	15	22	24	>50	ND
C4 position						
D-Tagatose	2.5	7.5	71	18	>50	ND
C5 position						
L-Sorbose	4	1	93	2	>50	ND
C6 position						
D-Xylulose	63	20	—	—	>50	ND

Values are in mM unless otherwise indicated. Independent replicate K_i values based on inhibition of D-glucose uptake are shown. Proportions of different forms are from published work (29). The proportion of acyclic carbonyl forms is omitted.
*Means ± SE of three independent experiment

BIOCHEMISTRY

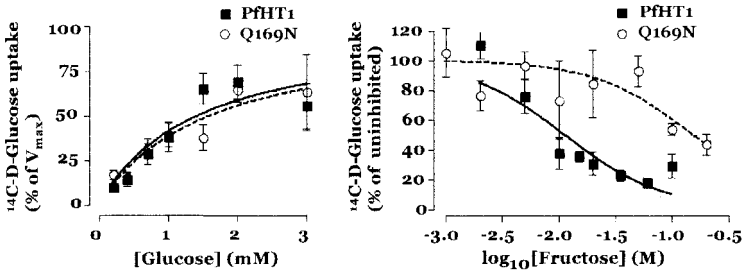

Fig. 4. Transport properties of Q169N mutant PfHT1. (*Left*) Initial mean D-glucose uptake rates for PfHT1 and Q169N mutant (one of three independent experiments in each case; eight oocytes per concentration; mean ± SE). For PfHT1 in this experiment, K_m = 1.6 mM, V_{max} = 302 pmol/oocyte/h; for Q169N K_m = 1.4 mM, V_{max} = 650 pmol/oocyte/h. (*Right*) D-fructose inhibition of D-[^{14}C]glucose uptake in PfHT1 and Q169N mutant. Uptakes (eight oocytes per concentration; mean ± SE) are expressed relative to D-glucose uptake in uncompeted oocytes.

there is sufficient room in the ligand-binding pocket of PfHT1 to accommodate the C3 methyl group.

Epimer Analysis. There are three epimers of D-glucose, each of which has an axial rather than equatorial hydroxyl at asymmetric carbons (positions 2, 3, or 4). D-mannose (the C2 epimer) has a K_i similar to that of D-glucose, consistent with the lack of significant hydrogen bond requirement at C2 (Table 1). In contrast, D-allose (the C3 epimer) competes poorly for glucose uptake mediated by PfHT1, demonstrating the importance of bonding by the axially placed hydroxyl at C3. The intermediate K_i of D-galactose (the C4 epimer) suggests that the equatorially orientated 4-hydroxyl of D-glucose is involved in hydrogen bonding that is weakened (or sterically hindered) in an axial orientation.

Aldopentose Analysis. D-xylose, which has a ring structure virtually identical to D-glucose but lacking a C6 carboxyl group, has a much lower affinity than 6-DOG for PfHT1. These results indicate a steric requirement for C6 independent of hydrogen bonding (Table 1).

D-Fructose and Ketose Analogues. D-Fructose consists of three major cyclic forms with 25–30% in the furanose form (Table 2). 2,5-Anhydro-D-mannitol (2,5-AHM, 2-deoxy-β-fructofuranose) is a useful analogue of β-fructofuranose, because it is a fixed furanose ring differing only in the absence of a 2-hydroxyl group. 2,5-AHM is a high-affinity inhibitor of D-glucose uptake (Table 2, K_i = 1.4 ± 0.3 mM), showing that the β-furanose form of fructose binds PfHT1. α-L-Sorbopyranose, which makes up >95% of L-sorbose, differs from D-fructopyranose only in the equatorial orientation of its C5 hydroxyl (the C2 equivalent in glucopyranose). L-Sorbose failed to inhibit glucose transport, suggesting that fructose is not transported in a fructopyranose form by PfHT1, although changes in the orientation of the C5 hydroxyl group may also be important for binding. The 3-epimer of D-fructose, D-psicose, existing as >50% furanose (Table 2), also failed to inhibit glucose transport.

Other Ligands. D-mannitol and D-sorbitol, analogues of the open (carbonyl) form of D-glucose, failed to inhibit glucose transport by PfHT1 (Table 1), proving that only cyclic forms bind to the transporter. 4,6-*O*-ethylidene-α-D-glucose, an exofacial binding-site probe previously used in studies on GLUT1 (6, 12), shows poor affinity for PfHT1 (K_i > 50 mM). DHA, a precursor of vitamin C that is transported by GLUT1 and GLUT3 with relatively high affinity (10), competed poorly with glucose for transport by PfHT1 (K_i > 50 mM).

GLUT1. GLUT1 sequences from different mammalian sources and their functions are highly conserved (13). In our studies, the K_m for D-glucose transport by GLUT1 is approximately 2.5 mM (Table 1), comparable to previously reported estimates [e.g., 1.6 mM for net influx (13)]. To compare PfHT1 and GLUT1, we have used hexose analogues to examine the substrate specificity of GLUT1 (Tables 1 and 2). For substitutents at many carbon positions, changes in K_i values are similar in magnitude to those seen with PfHT1. For example, hydroxyl groups at the C1 and C3 positions are crucial to interactions with GLUT1 as previously observed (14), whereas 2-DOG remains a high-affinity competitor for both transporters. However, clear differences between PfHT1 and GLUT1 also emerge. 3-OMG is a relatively poor competitive inhibitor of GLUT1 (K_i > 30 mM), having >10-fold lower affinity for GLUT1 than D-glucose. This relatively decreased affinity distinguishes GLUT1 from PfHT1 where 3-OMG competes with high affinity. The >6-fold increase in K_i observed for 6-DOG for GLUT1 (compared with the K_m for glucose) indicates that hydrogen bonding at the 6-position is more important in GLUT1 than PfHT1.

The most profound difference between PfHT1 and GLUT1 lies in the inability of GLUT1 to accept D-fructose; the fixed furanose ring analogue 2,5-AHM fails to inhibit D-glucose transport by GLUT1, confirming that GLUT1 does not accept a furanose form.

Mutational Analysis of PfHT1. The effects of changing Q169 of PfHT1 to an asparagine residue (Q169N) were examined in *Xenopus* oocytes. The affinity of glucose for Q169N is K_m = 1.2 ± 0.2 mM in three independent experiments and is similar to that for native PfHT1 (P = 0.67; Student's t test). In contrast, Q169N mutation abolished fructose transport and increased the K_i for fructose inhibition of glucose transport from 11.5 mM to >150 mM (>10-fold increase; Fig. 4 *Right*). Similarly, the K_i for 2,5-AHM increased from 1.4 mM to 28 mM in the mutant (>15-fold increase). Binding by the mutant to the C1 position in pyranoses was comparable to native PfHT1; 1F1α-DOG and 1F1β-DOG (both 10 mM) inhibited glucose uptake by >75% (not shown).

***In Vitro* Cultures of *P. falciparum*.** To investigate the role of fructose in parasite development during the erythrocytic cycle, infected erythrocytes were cultured with hexoses selected on the basis of results obtained with heterologous expression studies on GLUT1 and PfHT1 (Fig. 5). Even with relatively low initial parasitemias (0.3%), increasing glucose (from 20 to 40 mM) stimulated [^{3}H]hypoxanthine incorporation by ≈20% (P < 0.0001), an increase comparable to that observed when 20 mM fructose was added to 20 mM glucose (P = 1 comparing increases between supplementation with 20 mM glucose and 20 mM fructose).

To test whether fructose could replace glucose as a source of energy for parasites, medium containing negligible glucose (≈0.5 mM) was supplemented with increasing concentrations of

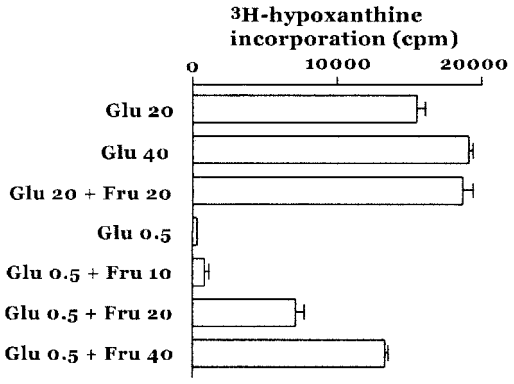

Fig. 5. *In vitro* studies on *P. falciparum* by using hexose analogues. Standard culture medium contains ≈20 mM D-glucose (Glu 20). The effects of supplementing this medium on [^{3}H]hypoxanthine incorporation with glucose (Glu 40; final concentration 40 mM D-glucose); fructose (Fru 20; D-fructose 20 mM) are shown (*Upper*). The effects of culture in 0.5 mM glucose (Glu 0.5; containing 10% human serum and glucose-free RPMI 1640), and of increasing concentrations of D-fructose supplements (Fru 10, 20, and 40; respectively 10 mM, 20 mM, and 40 mM fructose) are shown (*Lower*). Representative of three independent experiments.

fructose. Fructose supplementation (40 mM) successfully restores parasite growth limited by absence of glucose, whereas 20 mM fructose only partially restores parasite growth (46%; $P < 0.0001$ compared with 20 mM glucose).

Discussion

Severe malaria infection is associated with a high mortality (≈20%) despite appropriate treatment with conventional antimalarials. Mortality is highest in the first 24 h after admission (15). Conventional antimalarials require many hours to inhibit parasite glycolysis significantly (11) so that glucose consumption and lactic acid production continue and may perturb metabolism of host cells wherever infected erythrocytes obstruct microvasculature. In these circumstances, there is an urgent need to identify adjunctive therapies that can be used alongside antimalarial treatment to reduce mortality from severe malaria (15).

Inhibition of PfHT1 is predicted to confer two advantages to existing antimalarial therapy. First, immediate cessation of glycolytic activity by parasites may prevent diversion of glucose from host tissues whenever delivery of glucose is rate limiting (4). These conditions apply when anaerobic glycolysis by, for example, cerebral tissues, is increased by reduced oxygen delivery because of obstruction of capillaries by infected erythrocytes. Second, killing of parasites may take place more rapidly after exposure to inhibitors of PfHT1 than after exposure to antimalarials alone. Parasite ATP levels fall immediately after glucose supply is interrupted, confirming that asexual-stage parasites lack significant energy stores and are critically dependent on glucose, particularly for regulation of pH (1, 16).

Differences between host and malarial facilitative hexose transporters can be mapped by using a robust heterologous expression system. We began by defining important sequence elements in untranslated regions that contribute to efficient expression of PfHT1. Both a strong eukaryotic Kozak consensus sequence and untranslated 5′ and 3′ elements enhance expression of PfHT1 in *Xenopus* oocytes, and a combination of these features acts synergistically (Fig. 1). It is likely that introducing a strong Kozak consensus sequence and appropriate choice of vector will also prove important in the study of other malarial transport proteins, as many malarial-encoded sequences lack a strong Kozak consensus sequence.

In humans, only GLUT5 can mediate uptake of fructose with comparable affinity to PfHT1 (17). Site mutagenesis studies (discussed below) demonstrate that fructose transport capability has evolved through distinct mechanisms (i.e., convergently). D-fructose inhibits transport by PfHT1 of D-glucose with a $K_i \approx$ 11 mM (comparable to the K_m for fructose), suggesting that both hexoses are translocated through a common hexose permeation pathway. A wide range of glucose analogues has defined hydrogen-bond sites between PfHT1 and the six-membered pyranose ring of glucose (Table 1). The most important hydrogen bonds are between PfHT1 and hydroxyl groups at C1 and C3 in glucose. The C1-hydroxyl maintains this bond in both the α and β configurations. Hydroxyls at other positions appear less important in binding, because their removal or reorientation has relatively little effect on affinity. However, although the C4–C6 side of the glucose molecule may have little part to play in hydrogen-bond formation, there are tight constraints on its steric properties. Removal of C6 itself reduces affinity by approximately 10-fold compared with 6-DOG.

Analysis of interaction with fructose is more complicated, because this ketose exists as a mixture of pyranose and furanose forms in solution. Ketose analogues provide clear evidence that fructose binds to PfHT1 in the furanose form. In a fructose solution with concentration equivalent to K_i (≈11 mM), β-fructofuranose is predicted to be at a concentration of ≈2 mM. The K_i of the fixed β-fructofuranose analogue 2,5-AHM (1.4 mM) is similar to this value, suggesting that binding of D-fructose to PfHT1 (and presumably subsequent transport) takes place in the furanose form as observed with *Trypanosoma brucei* (18). In support of this hypothesis, the ketose analogue L-sorbose existing almost exclusively as pyranose binds poorly to PfHT1. Hydrogen bonding at the C2 position is not important, because 2,5-AHM (2-deoxy-β-fructofuranose) binds with high affinity. In contrast, the 3-epimer of D-fructose, D-psicose also forms furanose-rich solutions, yet binds poorly to PfHT1.

An active analogue analysis has also been applied to several kinetoplastid transporters that can transport glucose and fructose. Compared with PfHT1, there is greater reliance on the C6 position to mediate hydrogen bonding, with less importance attached to the C1 position.

We have expressed GLUT1, the major erythrocyte and blood–brain barrier transporter, in parallel with PfHT1. Active analogue analysis indicates there is emphasis on hydrogen bonding to the C1 and C3 positions for GLUT1, as previously described. However, we also noted significant differences between PfHT1 and GLUT1. 3-OMG binds with much higher affinity to PfHT1 than GLUT1, whereas GLUT1 is more reliant than PfHT1 on the C6 hydroxyl. The vitamin C analogue DHA is transported at high affinity by GLUT1 and GLUT3 (10) (transporters that are incapable of fructose transport) but not GLUT2 or GLUT5 (fructose transporters). Our finding that DHA fails to bind to PfHT1 therefore extends the mutual exclusivity of fructose and DHA transport to include PfHT1.

Site-directed mutagenesis studies have already provided information on structure/function relationships in GLUT1 (6, 19–21), whereas cysteine-scanning mutagenesis of GLUT1 helix 5 has confirmed predictions, derived from analysis of primary sequence, that this helix is amphipathic in nature (22, 23). In concert with other transmembrane segments, helix 5 may form a pore-like structure into which exofacial substrate passes. The external solution can access several amino acids within helix 5 of GLUT1, the deepest of which is predicted to be Q161. When this amino acid was mutated to an asparagine residue, the exofacial binding site was affected (6). A corresponding mutation in the *Chlorella* H^+-dependent glucose transporter (HUP1) increased the K_m for glucose 10-fold (7). As these proteins are specific for glucose, mutational analysis could not include other substrates such as fructose.

Secondary structure analysis of PfHT1 also predicts an amphipathic transmembrane helix 5. In addition, clusters of amino acids on the hydrophilic face of the helix are identical to equivalents in GLUT1 including Q169, which we mutated to an asparagine residue. This Q169N mutant continued to transport D-glucose, with a K_m comparable to that of wild-type PfHT1 (Fig. 4). Fructose transport was abolished and the K_i for fructose increased by >10-fold. There was a similar increase in the K_i for the fixed furanose analogue 2,5-AHM, confirming loss of furanose binding. The mechanism by which shortening of the polar amino acid side chain of Q169 leads to such a profound reduction in furanose binding needs clarification, for example, by introducing different amino acid residues at this site. Work on mammalian glucose transporters suggested that distinction between glucose and fructose is determined by sequences in transmembrane helices 7 and 8, and in particular a tripeptide motif in helix 7 (24, 25). Our findings establish that a single residue in helix 5 is a key determinant of fructose transport in PfHT1.

Intraerythrocytic parasites meet most of their glucose requirements via GLUT1, as assessed by kinetic studies on infected erythrocytes (1). A previous study examined fructose (≈10 mM) as a replacement for glucose in cultured parasites (26) and showed that growth was ≈75% and 25% after 24 h and 48 h, respectively, compared with controls. Our observations are consistent with these reports and suggest that much higher concentrations of fructose than 10 mM are needed to maintain parasite development (Fig. 5).

A combination of heterologous expression studies and experiments on asexual stage parasites has allowed us to put forward a detailed model summarizing hexose permeation pathways of intraerythocytic parasites. This model is consistent with previous studies on hexose transport observed in infected and uninfected erythrocytes. Glucose and fructose cross the erythrocyte plasma membrane via GLUT1 and GLUT5, respectively (17, 23); in mature stages of parasite development, these hexoses may additionally enter novel permeation pathways (1, 27). Substrates cross the parasitophorous vacuolar membrane via relatively nonselective channels (28). Both glucose and fructose may enter the parasite through PfHT1 located in the parasite plasma membrane.

We thank Drs. Michael Barrett and Kevin Saliba for discussion and Professor Gwyn Gould for the pSPGT1 construct. C.J.W. is a Wellcome Trust Clinical Training Fellow, and S.K. is a Wellcome Trust Senior Research Fellow in Clinical Science.

1. Kirk, K., Horner, H. A. & Kirk, J. (1996) *Mol. Biochem. Parasitol.* **82,** 195–205.
2. Woodrow, C. J., Penny, J. I. & Krishna, S. (1999) *J. Biol. Chem.* **274,** 7272–7277.
3. Pardridge, W. M. & Boado, R. J. (1993) in *The Blood–Brain Barrier: Cellular and Molecular Biology*, ed. Pardridge, W. M. (Raven, New York), pp. 395–440.
4. Krishna, S. & Woodrow, C. J. (1999) in *Transport and Trafficking in the Malaria-Infected Erythrocyte*, ed. Cardew, G. (Wiley, London), Vol. 226, pp. 126–144.
5. Kaback, H. R. (1996) in *Transport Processes in Eukaryotic and Prokaryotic Organisms*, eds. Konings, W. N., Kaback, H. R. & Lolkema, J. S. (Elsevier, Amsterdam), Vol. 2, pp. 203–227.
6. Mueckler, M., Weng, W. & Kruse, M. (1994) *J. Biol. Chem.* **269,** 20533–20538.
7. Caspari, T., Stadler, R., Sauer, N. & Tanner, W. (1994) *J. Biol. Chem.* **269,** 3498–3502.
8. Gould, G. & Lienhard, G. E. (1989) *Biochemistry* **28,** 9447–9452.
9. Penny, J. I., Hall, S. T., Woodrow, C. J., Cowan, G., Gero, A. M. & Krishna, S. (1998) *Mol. Biochem. Parasitol.* **93,** 81–89.
10. Rumsey, S. C., Kwon, O., Xu, G. W., Burant, C. F., Simpson, I. & Levine, M. (1997) *J. Biol. Chem.* **272,** 18982–18989.
11. ter Kuile, F., White, N. J., Holloway, P. H., Pasvol, G. & Krishna, S. (1993) *Exp. Parasitol.* **76,** 85–95.
12. Hashiramoto, M., Kadowaki, T., Clark, A., Muraoka, A., Momomura, K., Sakura, H., Tobe, K., Akanuma, Y., Yazaki, Y., Holman, G. & Kasuga, M. (1992) *J. Biol. Chem.* **267,** 17502–17507.
13. Gould, G. & Holman, G. D. (1993) *Biochem. J.* **295,** 329–341.
14. Carruthers, A. & Zottola, R. J. (1996) in *Transport Processes in Eukaryotic and Prokaryotic Organisms*, eds. Konings, W. N., Kaback, H. R. & Lolkema, J. S. (Elsevier, Amsterdam), Vol. 2, pp. 311–342.
15. Newton, C. R. & Krishna, S. (1998) *Pharmacol. Ther.* **79,** 1–53.
16. Saliba, K. J. & Kirk, K. (1999) *J. Biol. Chem.* **274,** 33213–33219.
17. Concha, I. I., Velasquez, F. V., Martinez, J. M., Angulo, C., Droppelmann, A., Reyes, A. M., Slebe, J. C., Vera, J. C. & Golde, D. W. (1997) *Blood* **89,** 4190–4195.
18. Fry, A. J., Towner, P., Holman, G. D. & Eisenthal, R. (1993) *Mol. Biochem. Parasitol.* **60,** 9–18.
19. Hresko, R. C., Kruse, M., Strube, M. & Mueckler, M. (1994) *J. Biol. Chem.* **269,** 20482–20488.
20. Garcia, J. C., Strube, M., Leingang, K., Keller, K. & Mueckler, M. M. (1992) *J. Biol. Chem.* **267,** 7770–7776.
21. Mueckler, M. & Makepeace, C. (1997) *J. Biol. Chem.* **272,** 30141–30146.
22. Mueckler, M. & Makepeace, C. (1999) *J. Biol. Chem.* **274,** 10923–10926.
23. Mueckler, M., Caruso, C., Baldwin, S. A., Panico, M., Blench, I., Morris, H. R., Allard, W. J., Lienhard, G. E. & Lodish, H. F. (1985) *Science* **229,** 941–945.
24. Seatter, M. J., De La Rue, S., Porter, L. M. & Gould, G. W. (1998) *Biochemistry* **37,** 1322–1326.
25. Wu, L., Fritz, J. D. & Powers, A. C. (1998) *Endocrinology* **139,** 4205–4212.
26. Geary, T. G., Divo, A. A., Bonanni, L. C. & Jensen, J. B. (1985) *J. Protozool.* **32,** 608–613.
27. Kirk, K., Horner, H., Elford, B. C., Ellory, J. C. & Newbold, C. I. (1994) *J. Biol. Chem.* **269,** 3339–3347.
28. Desai, S. A., Krogstad, D. J., Lambros, C., Kelley, W. N. & Webster, H. K. (1997) *Proc. Natl. Acad. Sci. USA* **94,** 2045–2049.
29. Collins, P. M. & Ferrier, R. J. (1995) *Monosaccharides* (Wiley, Chichester, U.K.).